JOURNAL OF THERMOPHYSICS AND HEAT TRANSFER
Vol. 11, No. 4, October–December 1997

Impact of Nucleation Density on Thermal Resistance near Diamond-Substrate Boundaries

M. N. Touzelbaev* and K. E. Goodson†
Stanford University, Stanford, California 94305-3030

The measured thermal resistance between deposited layers and substrates at room temperature is not well predicted by existing theory. This may result, in part, from microstructural disorder in the deposited film within tens of nanometers of the interface. The present manuscript develops a model for the thermal resistance near diamond-substrate interfaces, where the best deposition processes continue to yield high concentrations of amorphous inclusions and nanocrystalline material. The model relies on phonon transport theory and a novel subdivision of the near-interfacial region, which shows that the resistance is governed by the number of diamond nucleation sites per unit substrate area, i.e., the nucleation density. The predictions are consistent with experimental data for diamond–silicon interfaces, and indicate that the resistance reaches a minimum for a nucleation density near 10^{10} cm^{-2}. This work facilitates the development of microstructures that benefit more strongly from the excellent thermal-conduction properties of diamond.

Nomenclature

A_U = fitting parameter for relaxation time of phonon–phonon scattering, s^{-1} K^{-3}
B_U = fitting parameter for relaxation time of phonon–phonon scattering, K
C_V = phonon specific heat per unit volume, J m^{-3} K^{-1}
D_{RC} = diameter of extended defects, m
d = characteristic grain dimension, m
d_h = fitting parameter for diamond thermal conductivity, m
d_0 = initial characteristic grain dimension, m
f_d = crystalline diamond area fraction
h_P = Planck's constant divided by $2\pi = 1.06 \times 10^{-34}$ J s
k = thermal conductivity, W m^{-1} K^{-1}
k_a = thermal conductivity of amorphous material, W m^{-1} K^{-1}
k_B = Boltzmann constant, 1.38×10^{-23} J K^{-1}
k_d = thermal conductivity of diamond, W m^{-1} K^{-1}
k_{db} = thermal conductivity of bulk diamond, W m^{-1} K^{-1}
$n_{GB,j}$ = number of defects of type j per unit grain boundary area, m^{-2}
R = thermal resistance, m^2 K W^{-1}
R_B = effective thermal boundary resistance, m^2 K W^{-1}
T = temperature, K
V_0 = volume of the host atom in expression for Rayleigh scattering, m^3
v_s = average phonon velocity, ms^{-1}
x, y = coordinates along the layer, m
x_ω = nondimensional phonon angular frequency
z = coordinate normal to layer, m
z_B = thickness of near-interfacial region with increased temperature gradients, m
z_L = layer thickness, m
z_N = nucleation height, m
γ = diamond spatial grain-size gradient near the deposition boundary
Δz_C = thickness of grain closure region, m
Δz_R = thickness of randomly oriented grain region, m
δ = length-scale of imperfection concentration near grain boundaries, m
η = grain boundary scattering strength
θ_D = Debye temperature of diamond, K
ρ = nucleation density, m^{-2}
σ_j = cross section for phonon scattering on defects of type j, m^2
τ = phonon relaxation time, s
τ_{GB} = phonon relaxation time because of grain boundaries, s
τ_U = phonon relaxation time because of Umklapp processes, s
ω = phonon angular frequency, s^{-1}

Received Sept. 3, 1996; revision received Feb. 26, 1997; accepted for publication April 4, 1997.
*Research Assistant, Mechanical Engineering Department.
†Assistant Professor, Mechanical Engineering Department.

I. Introduction

THE exceptional properties of diamond promise to make electronic devices with unprecedented figures of merit possible. The potential devices include transistors made from composite silicon–diamond substrates,[1] high-temperature diamond thermistors,[2] and laser diode arrays mounted on diamond microchannel heat sinks[3]. These devices benefit from the large thermal conductivity of diamond, which exceeds 2000 W m^{-1} K^{-1} in bulk samples at room temperature. The small required quantities of diamond are relatively cheap to deposit, and the diamond thermal conductivity offers a vast improvement over that of alternative passivation materials, such as silicon–dioxide. But the deposition of diamond on nondiamond substrates yields a highly imperfect structure near the interface, which is evidenced by the small grains in the top-view electron micrographs shown in Fig. 1. Recent data[4] showed that this microstructural disorder yields a thermal resistance that can strongly impede conduction cooling. The thermal resistance is dominated by the contribution resulting from disorder within tens of nanometers of the diamond–substrate interface. There is little theory and data available that examine the thermal resistance caused by disorder near interfaces, between the deposited layers and substrates.

Thermal conduction analysis usually distinguishes between volume and boundary resistances. These two types of resistances are not truly distinct, because all boundary resistances can be described using increased temperature gradients over a region of finite dimensions (Fig. 2). The thickness of this region depends on the physical situation at the interface that is

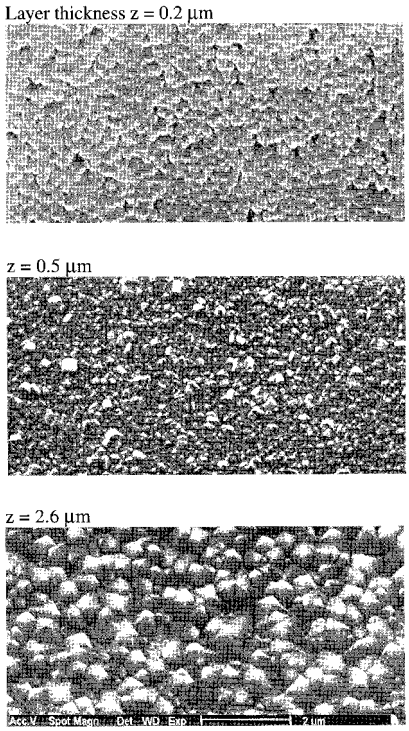

Fig. 1 Top-view electron micrographs of diamond layers deposited on silicon. The coordinate z is normal to the substrate-layer interface.

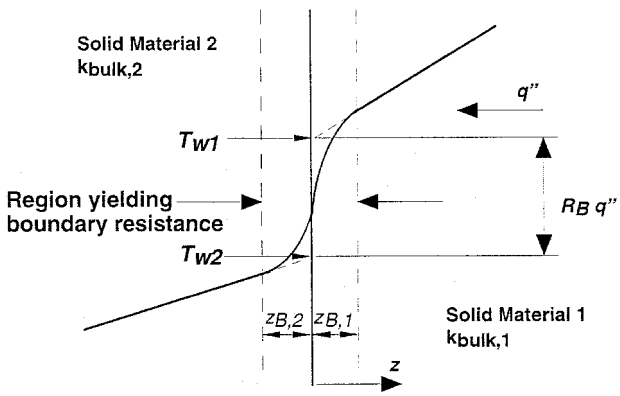

Fig. 2 Schematic of the temperature distribution near solid–solid boundary. For acoustic-mismatch theories, the thicknesses z_B values are of the order of phonon mean free paths in the two materials. For incomplete contact theories, the z_B are comparable with the surface roughness. For the present study, z_B is governed by the thickness of highly disordered material.

dominating the resistance, such as a) incomplete contact between the media, b) mismatch of acoustic properties, or c) microstructural disorder. For case a, the thickness of the region with increased temperature gradients is governed by the surface roughness for optically or nominally flat surfaces, and by the profile flatness deviation or the radius of curvature for non-flat surfaces. For case b, the thickness is determined by the mean free paths of heat carriers in the two materials. For case c, the thickness is governed by the extent of the microstructural disorder near the interface. When the dimensions of the media being modeled are much larger than the thickness of the region governing the boundary resistance, it is useful and appropriate for engineering design calculations to model this region using a thermal boundary resistance.

Much experimental and theoretical research has investigated the resistance caused by incomplete contact between media.[5–8] Many of these theories relate boundary resistance to the applied compressive pressure and the topography of the surfaces of the two media. Another approach accounts directly for surface topography by using fractal geometry to estimate the actual contact area of nominally flat surfaces from data.[9] Because many deposited thin films adhere to substrates on an atomic scale, incomplete contact theories are inappropriate for describing the thermal boundary resistance at film–substrate interfaces.

There is also a large body of research that has investigated the boundary resistance caused by the mismatch of acoustic properties at an interface.[10,11] Reasonable agreement is observed with data at temperatures below about 30 K, where the dominant wavelength of phonons is considerably longer than the typical length-scales of interfacial roughness. Acoustic-mismatch theory generally yields predictions that are too low at room temperature for most deposited layers. This is caused, in part, by near-interfacial disorder,[11] for which very little detailed modeling has been performed. Some of the discrepancy between acoustic-mismatch predictions and data near room temperature may result from the departure of the phonon dispersion relationships in the media from the linear model of Debye. For highly polished surfaces that are smooth on an atomic scale, Stoner and Maris[12] showed that the resistance resulting from acoustic mismatch can be detected at room temperature, where its value becomes very small, as predicted by theory. Such perfect interfaces can rarely be achieved in practice. Therefore, a study of thermal resistance caused by interface disorder is of practical importance.

Morath et al.[13] studied thermal properties of very thin diamond and diamond-like-carbon (DLC) films. They observed that the conductivities of DLC films are well modeled, using the Einstein theory for the lattice specific heat, which was assumed to be appropriate for the description of energy transfer between atoms not arranged in a periodic structure. In contrast, the same authors[13] showed that the use of the Einstein theory significantly underpredicts the measured thermal conductivity of diamond films, which is better modeled using the Debye theory for the lattice specific heat.[14] Stoner et al.[15] showed that near the substrate boundary, diamond films contain an amorphous mixture of substrate and carbon atoms together with diamond microcrystallites. There has been little progress on the modeling of thermal resistance of such composite layers.

The present manuscript develops a boundary-resistance theory that accounts for disorder near an interface. For this theory, the increased temperature gradients occur within a region of thickness comparable to that of the disorder. The boundary resistance is defined in a manner similar to that used for acoustic-mismatch and incomplete contact theories, i.e., by means of the relationship between the heat flux and the projected temperature drop (Fig. 2). In this work, the details of the theory are tailored to diamond–substrate interfaces, where this type of resistance is particularly important. The model relies on phonon transport theory and a novel subdivision of the near-interfacial region that is consistent with electron micrographs of diamond thin films. The resistance is calculated as a function of the nucleation density of grains, the slope of increase of grain size with the separation from the substrate, and the concentration of imperfections near grain boundaries. These parameters are extracted from top- and side-view electron micrographs and thermal-conductivity data for bulk samples. The predictions are consistent with data investigating thermal conduction normal to diamond layers deposited on silicon. This model helps tailor deposition parameters to minimize the thermal boundary resistance. In addition, this study provides the groundwork for a more general model of thermal boundary resistance caused by near-interfacial disorder.

Section II develops the microstructural subdivision of the near-interfacial region. Section III models the thermal boundary resistance in the subregions, using a model for the phonon-scattering rate within diamond that is discussed in Sec. IV. The

results are presented in Sec. V along with a comparison with experimental data.

II. Subdivision of the Near-Interfacial Disordered Region

The top-view electron micrographs in Fig. 1 show chemical vapor deposited (CVD) diamond layers of varying thicknesses fabricated using identical deposition process. The micrographs illustrate changes in the diamond grain structure, with increasing distance from the deposition interface. The grains grow rapidly in the lateral dimension with increasing separation from the substrate. The changing grain size is largely responsible for the spatial variation of the thermal-conduction properties. This section develops a novel subdivision of this disordered region. The subdivision (Fig. 3), uses assumptions that are justified by the electron micrographs in Fig. 1, the detailed characterization work for diamond–silicon interfaces performed by Stoner,[15] and the observations about the diamond grain structure of Goodson.[16]

The initial diamond growth yields an amorphous layer of mixed stoichiometry of thickness comparable to $z_N = 50$ Å. The layer consists of noncrystalline and nanocrystalline combinations of carbon and substrate atoms. Stoner et al.[15] observed this layer for diamond deposited on silicon, and hypothesized that it is required for nucleation. As this layer grows, an increasing fraction of incident atoms remains at the surface, forms clusters, and provides nucleation sites for diamond grains. The nucleation of diamond occurs at distances from the interface usually not greater than $z_N = 100$ Å. However, transmission electron micrographs of layers fabricated by other groups have suggested that diamond crystals can nucleate directly on silicon, i.e., $z_N \sim 0$. Avoiding the formation of this sublayer is desirable for passive applications of diamond, not only because of its poor thermal conduction properties, but also because of its low electrical resistivity. In each particular case, the choice of z_N needs to be based on microstructural information obtained for the layers under study.

In the second region, $z_N < z < z_N + \Delta z_C$, the nucleated grains grow in lateral dimension, with increasing distance from the substrate. The region between grains is filled with amorphous material of stoichiometry, increasingly dominated by carbon with increasing z. The thickness Δz_C depends on the nucleation density and the crystal growth angle. This angle describes the departure of opposing grain walls from one another with increasing z, and is approximately 90 deg for grains with ⟨100⟩ orientation. Growth processes yielding textured layers eventually favor a single orientation. The closure height, $z_N + \Delta z_C$, is defined here as the position at which the diamond grains close over the substrate, preventing further growth of the amorphous regions.

After closure, $z > z_N + \Delta z_C$, the grains cannot continue to grow freely in the lateral dimension. Some of the grains terminate, while others grow larger. The resulting orientation of grain boundaries is practically random. While the thermal conductivity of this region is considerably larger than that of the region below the closure height, which contains amorphous material, it is much less than that of bulk diamond because of the small grain size. Goodson[16] modeled the increase of the thermal conductivity of diamond with increasing values of the local grain dimension d. The characteristic grain dimension is defined for a given x-y plane as the average separation between intersections of a reference line with grain boundaries in that plane. The smallest grain dimension in this region, d_o, occurs at $z = z_N + \Delta z_C$. The structure of the grains eventually becomes columnar, as depicted at the height $z_N + \Delta z_C + \Delta z_R$ in Fig. 3, which leads to the textured structure observed in relatively thick layers. It is important to distinguish between grains with randomly oriented boundaries, which strongly impede heat flow normal to a substrate-film interface, and columnar grains, whose boundaries offer relatively little resistance to heat flow normal to a substrate-film interface.[16]

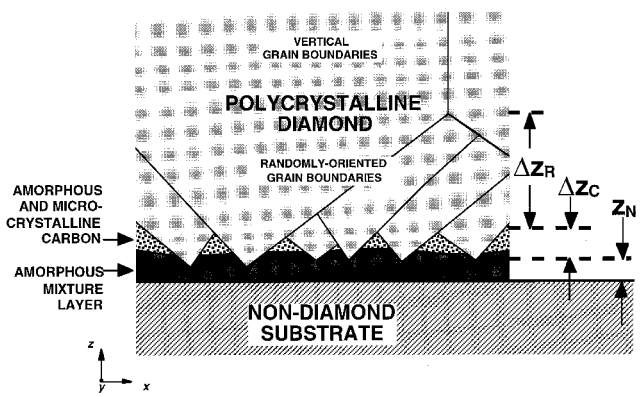

Fig. 3 Subdivision of the disordered region near diamond interfaces with nondiamond substrates.

III. Boundary Resistance Contributions

The resistance of each of the regions depicted in Fig. 3 is calculated using the heat-diffusion energy equation. This approach is justified by the small values of the mean free paths of phonon heat carriers compared to the modeled geometric length-scales. These length-scales include the average diamond grain size and the region thicknesses depicted in Fig. 3. To simplify the present treatment, temperature gradients in each x-y plane over the entire film are neglected compared to those in the z direction. This assumption makes each x-y plane isothermal, and results in an underprediction of the boundary resistance, since the spreading resistance is not considered. The error is caused primarily by the lateral conduction that occurs in the region with the greatest lateral nonhomogeneity, $z_N < z < z_N + \Delta z_C$. This error is expected to be small compared to those caused by the assumptions about the layer microstructure described in Sec. II.

The effective thermal boundary resistance is defined using the projected temperature drop at the interface, as depicted in Fig. 2, which yields

$$R_B = \frac{T_{w1} - T_{w2}}{q''} = \int_0^{\infty} \left[\frac{1}{k(z)} - \frac{1}{k_{\text{bulk},1}} \right] \mathrm{d}z + \int_{-\infty}^{0} \left[\frac{1}{k(z)} - \frac{1}{k_{\text{bulk},2}} \right] \mathrm{d}z \tag{1}$$

The conductivity $k(z)$ is the local value at position z, and approaches k_{bulk} as z approaches infinity. This conductivity is calculated differently for the different subdivisions in the near-interfacial region.

A. Prenucleation Region ($0 < z < z_N$)

Because of the large thermal resistance contribution of this prenucleation region, the choice of the thermal conductivity has a large impact on the predicted thermal boundary resistance. The required values of the thermal conductivity of disordered carbon mixtures have not been directly measured, and therefore the resistance of this region can at best be qualitatively determined but an estimate can be made based on its amorphous structure. Many amorphous solids have thermal conductivities comparable to 1 W m^{-1} K^{-1} at room temperature,[17,18] a value that does not vary strongly with the constituent atom. The thermal conductivity in this region is assumed to remain constant with all z at the value k_a.

B. Grain Closure Region ($z_N < z < z_N + \Delta z_C$)

This region consists of laterally growing diamond grains surrounded by amorphous material. The assumption of iso-

thermal conditions in each x-y plane allows the different materials to be treated in parallel, yielding

$$k(z) = k_d(z) f_d(z) + k_a[1 - f_d(z)] \tag{2}$$

where f_d is the area fraction in the x-y plane at z. The diamond conductivity k_d is coupled to the grain dimension using the theory described in Sec. IV.

C. Randomly Oriented Grain Region ($z_N + \Delta z_C < z < z_N + \Delta z_C + \Delta z_R$)

The characteristic grain dimension at $z = z_N + \Delta z_C$ is estimated by assuming that the grains are square in cross section in the x-y plane and are packed in a perfect periodic two-dimensional array. This idealization captures the approximate relationship between the nucleation density and the smallest grain dimension in the randomly oriented grain region

$$d_0 = 1.12/\sqrt{\rho} \tag{3}$$

The interpretation of Eq. (3) must consider the measurement technique for the grain dimension, which uses a reference list placed on a given x-y plane. Depending on the angle at which a reference line is drawn with respect to the sides of the square, the grain dimension varies from a value of $d_0 = \rho^{-0.5}$, if a reference line is parallel to the side to a value of $1.41 \cdot \rho^{-0.5}$, in case of the reference line coinciding with the diagonal of the square. The factor 1.12 results from averaging the grain dimension over all of the possible directions at which a reference line can be oriented with respect to the squares. The grain dimension is assumed to vary linearly with z according to

$$d = d_0 + \gamma(z - z_N - \Delta z_c) \tag{4}$$

The spatial grain-size gradient γ is calculated from top-view electron micrographs, which indicate that a linear dependence is approximately correct within a few micrometers of the substrate. A more detailed description is not appropriate because of the other approximations in the model. An approximate value of $\gamma = 0.2$ is consistent with the top-view electron micrographs in Fig. 1.

IV. Local Diamond Thermal Conductivity

This section summarizes the theory necessary to calculate the local thermal conductivity in diamond grains in the region $z > z_N$, as a function of the characteristic grain dimension. Goodson[16] provides a detailed description for heat transport calculations in CVD-diamond layers. An approximate solution to phonon Boltzmann transport equation yields the lattice thermal conductivity[19]

$$k = \frac{1}{3} v_s^2 \int_0^{\theta_D/T} C_V \tau \, \mathrm{d}x_\omega \tag{5}$$

where the phonon specific heat is

$$C_V = \frac{3k_B}{2\pi^2 v_s^3} \left(\frac{k_B T}{h_P}\right)^3 \frac{x_\omega^4 \exp(x_\omega)}{[\exp(x_\omega) - 1]^2} \tag{6}$$

The Debye temperature and average phonon velocity in diamond are $\theta_D = 2030$ K and $v_s = 13{,}200$ m s^{-1}, respectively. The total phonon scattering rate is

$$[\tau(d, \omega, T)]^{-1} = [\tau_U(\omega, T)]^{-1} + [\tau_{GB}(d, \omega)]^{-1} \tag{7}$$

Terms in Eq. (7) depend on ω, which governs the phonon scattering cross section, T, and d. The first term in Eq. (7), the Umklapp scattering rate, is modeled using[14]

$$[\tau_U(x_\omega, T)]^{-1} = A_U (x_\omega)^2 T^3 \exp[(-B_U)/T] \tag{8}$$

where $A_U = 640$ s^{-1} K^3, $B_U = 470$ K. The dimensionless phonon frequency is $x_\omega = h_P\omega/(k_B T)$.

The present work distinguishes between scattering on the boundaries of columnar and randomly oriented grains, because these influence the thermal resistance differently.[16] The scattering rate caused by randomly oriented grains assumes that imperfections associated with a given grain boundary are distributed uniformly within grains (model A), which yields a scattering rate that is proportional to the grain-boundary scattering strength and inversely proportional to the grain dimension

$$[\tau_{GB}(d, \omega)]^{-1} = 2 v_s \eta(d, \omega)/d \tag{9}$$

Columnar grains reduce the conductivity less strongly. This was considered by collapsing all of the imperfections onto the boundaries of grains (model B). This yielded

$$[\tau_{GB}(d, \omega)]^{-1} = \frac{2 v_s}{\pi d} \left\{1 - \exp\left[-\frac{\pi^2}{4} \eta(d)\right]\right\} \tag{10}$$

The dimensionless η is the fraction of the area of a grain boundary that induces phonon scattering, and is defined as

$$\eta(d, \omega) = \sum_{j=1}^{J} \sigma_j(\omega) n_{GB,j}(d) \tag{11}$$

Imperfections are considered using a scattering cross section[14]

$$\sigma_1(x_\omega, T) = \frac{V_0^2 x_\omega^4 T^4}{4\pi v_s^4} \left(\frac{k_B}{h_P}\right)^4 \tag{12}$$

for point defects, where $V_0 = 5.68 \times 10^{-30}$ m^3, and the cross section

$$\sigma_2(x_\omega, T) = \frac{\pi D_{RC}^6}{4 v_s^4} \left(\frac{k_B}{h_P}\right)^4 x_\omega^4 T^4 \quad \text{for} \quad x_\omega < \frac{h_P v_s}{k_B T D_{RC}}$$
$$= \frac{\pi (D_{RC})^2}{4} \quad \text{for} \quad x_\omega \geq \frac{h_P v_s}{k_B T D_{RC}} \tag{13}$$

for extended defects, e.g., groups of point defects or small regions with amorphous microstructure. The diameter of extended defects is approximated using $D_{RC} = 1.4 \times 10^{-9}$ m, and the number densities of defects per unit grain boundary area are approximated using $n_{GB,1} = 2.2 \times 10^{20}$ m^{-2} and $n_{GB,2} = 1.5 \times 10^{18}$ m^{-2} (Ref. 16).

Equation (9) shows that for the assumption of a uniform distribution of imperfections within grains (model A), the scattering rate grows arbitrarily large with increasing values of the scattering strength. But, Eq. (10) shows that if imperfections are collapsed on the grain boundaries (model B), the scattering rate has an upper bound dictated by the grain size. Thus, lower values of thermal conductivity are predicted by model A than by model B. The grain boundary scattering strength is assumed not to vary significantly within a given layer. The concentration of grain boundaries per unit volume depends strongly on the grain size.

The electron micrographs of Heatherington et al.[20] indicate that imperfections are concentrated near grain boundaries, within a thickness $\delta \sim 1000$ Å. When the grain dimension is smaller than or comparable to δ, model A is best suited for the thermal-conductivity calculation, because it distributes imperfections throughout the grain volume. When the grain dimension becomes considerably larger than δ, the scattering rate is better described using model B, which collapses imperfections onto the grain boundaries. This conclusion is valid only for layers with grains that approach columnar growth. For this range of grain dimensions, i.e., when d is somewhat larger than

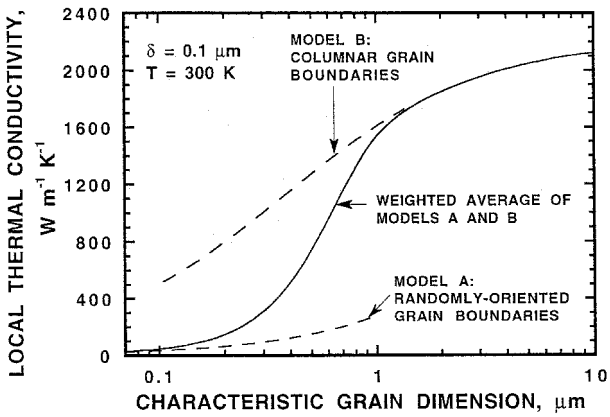

Fig. 4 Dependence of the local thermal conductivity on the characteristic grain dimension.

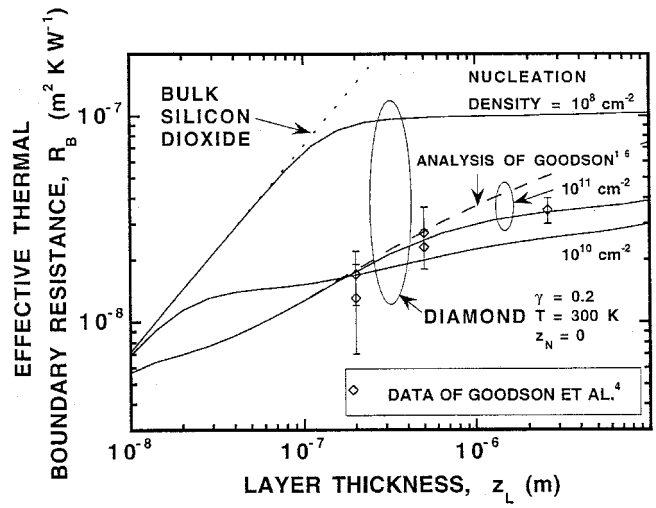

Fig. 5 Variation of the resistance normal to layers with nucleation density and film thickness.

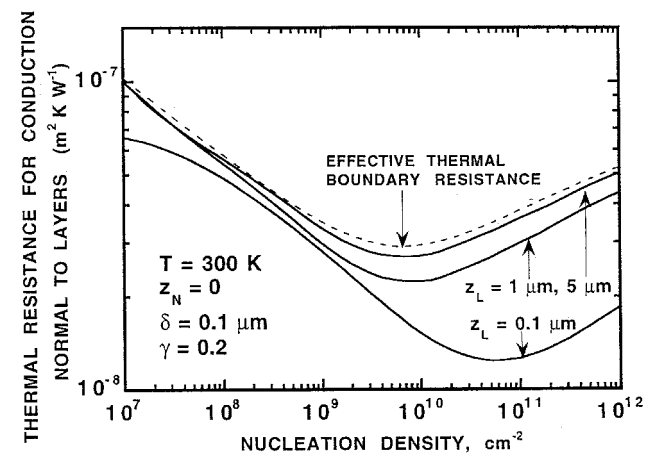

Fig. 6 Thermal resistance normal to layers as a function of nucleation density.

δ, neither model A nor model B is well suited. They provide lower and upper bounds for the thermal conductivity, respectively. In the intermediate regime, the thermal conductivity is estimated using a weighted average of the values calculated using models A and B, where the weighting functions are polynomials in d whose coefficients are chosen to yield $k = k_A$ at $d = \delta$ and $k = k_B$ at $d = 10\delta$ with continuous derivatives at these points. Figure 4 shows the result of this procedure.

V. Results and Discussion

Figure 5 shows the predicted dependence of the thermal resistance for conduction normal to layers on z_L for three values of the nucleation density. The thermal resistance at a given film thickness can be compared with measured values of the thermal resistance for conduction normal to a layer of that thickness. Data of this type were measured for gold–diamond–silicon sandwich structures by Goodson et al.[4] The nucleation density in that study was estimated to be in the order of 10^{11} cm^{-2}, which corresponds to a minimum grain dimension of 0.03 μm. The predicted resistances are consistent with the measured values considering the experimental uncertainty. The agreement is far better than that achieved through the phonon transport analysis of Goodson,[16] which did not account for the growing fraction of columnar grains in the layer with increasing z. The resistance of bulk silicon–dioxide, a common passive material in electronic applications, is shown on the same plot. Data for the thermal conductivity of thin silicon–dioxide films[21] indicate that the actual resistance can be considerably larger.

The impact of the nucleation density depends strongly on the layer thickness. The closure height governs the thickness of the highly resistive region containing amorphous material. Since the closure height increases with decreasing nucleation density, the resistance at low values of the thickness is greatest for low values of the nucleation density. But when layers with low nucleation density close, they have a high value of d_0, which results in a relatively small contribution of the region with randomly oriented grain boundaries to the resistance. This is responsible for the change in slope of the resistance relationship for the lowest nucleation density in Fig. 5. In contrast, layers with high nucleation densities (>10^{10} cm^{-2}) close at very small values of z and experience a gradual increase of the thermal conductivity with increasing z. For this reason, the resistance of layers with high nucleation density increases steadily with increasing film thickness. At a thickness near 1 μm, the conductivity from model B begins to dominate, which accounts for the transition to a columnar grain structure. Since columnar grains contribute relatively little to the thermal resistance, the resistance increases less rapidly with increasing z_L. We also observe that at thicknesses greater than about 0.1 μm, for layers in which the closure occurs before that thickness, the impact of the small value of d_0 begins to dominate, such that the resistance of layers with a high nucleation density is greater than that of layers with a low nucleation density.

It has been suggested that decreasing the nucleation density may reduce the layer thermal resistance by increasing the grain size near the deposition interface.[22] But a low nucleation density reduces the direct contact area between the diamond and the substrate and increases the volume fraction of amorphous material near the interface, both of which increase the effective boundary resistance. This suggests that the resistance reaches a minimum for some value of the nucleation density. The model developed in this study provides theory necessary to quantitatively describe this effect. This is illustrated by Fig. 6, which shows the dependence of the thermal resistance on the nucleation density for three values of the layer thickness. Indeed, the results indicate that for a given film thickness there is an optimum nucleation density that minimizes thermal resistance. The optimum nucleation density for thick films is near 10^{10} cm^{-2}. Figure 6 also shows the dependence of the thermal boundary resistance on the nucleation density, calculated using Eq. (1) in the manner depicted in Fig. 2. The boundary resistance is very close to the volume resistance of the first 5 μm of material near the interface. According to the new model, this region contains a large fraction of amorphous material and diamond grains with randomly oriented boundaries, thus contributing the most to the boundary resistance calculated according to Eq. (1).

The optimal nucleation densities are relatively high within the range achievable using common nucleation methods. The

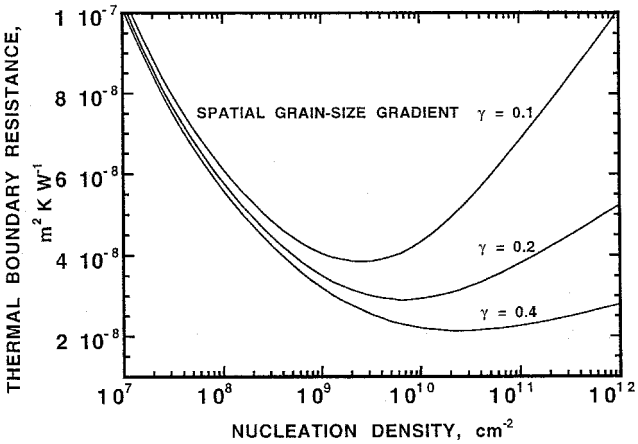

Fig. 7 Thermal boundary resistance as a function of nucleation density.

highest densities are common for layers nucleated using a bias voltage between the plasma source and the substrate, e.g., Stoner et al.[15] Lower nucleation densities are achieved using predeposition surface treatment, such as scratching. The optimum nucleation density decreases slightly with increasing layer thickness. This is explained by the growing contribution of a region with randomly oriented grain boundaries with increasing layer thickness. The smaller the contribution of this region, the smaller the impact of a small value of d_0 is on the total thermal resistance. This effect becomes small when the grains are predominantly columnar. Goodson et al.[4] estimated a nucleation density near 10^{11} cm^{-2} for their samples, which Fig. 5 shows to be consistent with the model developed here. The thermal resistance of these layers could be reduced by decreasing the nucleation density by about one order of magnitude.

Figure 7 demonstrates the importance of achieving the largest possible growth of grain dimension relative to the separation from the boundary. The large spatial lateral grain-size gradient results not only in a lower value of thermal boundary resistance, but also in an extension of the range of nucleation densities for which resistance is minimized.

To more clearly describe the competing phenomena that govern the optimum nucleation density in the model developed here, the resistances in the grain-closure region and randomly oriented grain region are approximated using closed-form algebraic expressions. The resistance of the grain-closure region is estimated using

$$R \sim 1/\sqrt{\rho}k_a \tag{14}$$

This models the closure region as an amorphous slab of thickness comparable to the average separation between nucleation sites. The resistance in Eq. (14) neglects the contribution of the diamond to thermal conduction in this region, but scales with the value obtained using Eqs. (1) and (2). Equation (14) is most accurate if the growth angle is comparable to 90 deg, which is the case for ⟨100⟩ oriented growth. The resistance of the randomly oriented grain region is governed by the height of the transition to columnar grain structure. This resistance can be estimated using the lowest thermal conductivity in the region, which occurs at $z = z_N + \Delta z_C$. This yields

$$R \sim \frac{10\delta}{\gamma k_d(z_N + \Delta z_C)} \tag{15}$$

where $10\delta/\gamma$ is the approximate height, and $k_d(z_N + \Delta z_C)$ is the minimum thermal conductivity in a slab resistance. This expression can be evaluated using an approximate fit to the dependence of the room-temperature diamond thermal conductivity on grain dimension, yielded by model A from Sec. IV

$$k_d(d) = k_{db}[d/(d + d_h)] \tag{16}$$

where $k_{db} = 2200$ W m^{-1} K^{-1}, and $d_h = 6 \times 10^{-6}$ m. The thermal conductivity $k_d(z_N + \Delta z_C)$ is evaluated using Eq. (16), given that the grain dimension at the coordinate $z = z_N + \Delta z_C$ is approximated according to Eq. (3) as $d = d_0 \sim \rho^{-1/2}$. The total boundary resistance is the sum of resistances given by Eqs. (14) and (15). The optimum nucleation density yields the zero of the derivative of the resistance

$$\rho_{min} \sim \frac{\gamma}{10 d_h \delta} \frac{k_{db}}{k_a} \tag{17}$$

While Eq. (17) does not capture all of the details of the present study, it provides a good approximation to the optimum nucleation density. For parameter values $\delta = 1000$ Å and $k_a = 1.4$ W m^{-1} K^{-1}, Eq. (18) yields $\rho_{min} = 5 \times 10^9$ cm^{-2}, which is consistent with the results in Fig. 6.

VI. Summary and Conclusions

This paper develops a model for the thermal resistance caused by microstructural disorder near the substrate interface of deposited layers near room temperature. The boundary resistance varies strongly with microstructural parameters, including the nucleation density and the spatial gradient of the grain dimension. The predictions of the model are consistent with data for the thickness-dependent thermal resistance of diamond layers on silicon. Previous studies suggested that thermal conduction near the diamond-substrate interface can be improved arbitrarily by decreasing the nucleation density, which increases the smallest grain size in the polycrystalline diamond near the interface. In contrast, the present work shows that for nucleation densities below about 10^{10} cm^{-2}, decreasing the nucleation density increases the volume of amorphous material near the interface, which actually impedes conduction. As a result of these competing effects, the model predicts that the thermal resistance of thin diamond layers reaches a minimum at a certain nucleation density for a value of the spatial grain-size gradient. This observation is important in choosing a deposition regime if a minimum normal thermal resistance is desired.

Many of the assumptions used in this study are tailored specifically for diamond layers deposited on nondiamond substrates. The guiding principles of this study, i.e., that the grain structure and volume fraction of amorphous material near an interface govern the effective boundary resistance, can be used to develop comparable theory for other technically important interfaces, such as those of polysilicon with metals and silicon–dioxide.

Acknowledgments

The authors appreciate the support of Daimler–Benz AG, Germany. K. E. Goodson acknowledges support from the Office of Naval Research Young Investigator Program and the National Science Foundation CAREER program. We thank O. W. Käding and H. Verhorven for providing valuable comments.

References

[1]Ravi, K. V., and Landstrass, M. I., "Silicon on Insulator Technology Using CVD Diamond," *1st International Symposium on Diamond and Diamond-Like Films*, edited by J. P. Dismukes et al., Electrochemical Society, Pennington, NJ, 1989, pp. 24–37.

[2]Werner, M., Schlichting, V., and Obermeir, E., "Thermistor Based

on Doped Polycrystalline Diamond Films," *Diamond and Related Materials*, Vol. 1, Nos. 5, 6, 1992, pp. 669–672.

[3]Goodson, K. E., Kurabayashi, K., and Pease, R. F. W., "Improved Heat Sinking in Laser-Diode Arrays Using Microchannels in CVD Diamond," American Society of Mechanical Engineers National Heat Transfer Conf., Portland, OR, Aug. 1995.

[4]Goodson, K. E., Käding, O. W., Rösler, M., and Zachai, R., "Experimental Investigation of Thermal Conduction Normal to Diamond-Silicon Boundaries," *Journal of Applied Physics*, Vol. 77, No. 4, 1995, pp. 1385–1392.

[5]Madhusudana, C. V., and Fletcher, L. S., "Contact Heat Transfer — The Last Decade," *AIAA Journal*, Vol. 24, No. 3, 1986, pp. 510–523.

[6]Yovanovich, M. M., "Recent Developments in Thermal Contact, Gap and Joint Conductance Theories and Experiment," *8th International Heat Transfer Conference*, edited by C. L. Tien, V. P. Carey, and J. K. Ferrel, Vol. 1, Hemisphere, New York, 1986, pp. 35–45.

[7]O'Callaghan, P. W., and Probert, S. D., "Thermal Resistance and Directional Index of Pressed Contacts Between Smooth Non-Wavy Surfaces," *Journal of Mechanical Engineering Science*, Vol. 16, No. 1, 1974, pp. 41–55.

[8]Cooper, M. G., Mikic, B. B., and Yovanovich, M. M., "Thermal Contact Conductance," *International Journal of Heat and Mass Transfer*, Vol. 12, No. 3, 1969, pp. 279–300.

[9]Majumdar, A., and Tien, C. L., "Fractal Network Model for Contact Conductance," *Journal of Heat Transfer*, Vol. 113, No. 3, 1991, pp. 516–525.

[10]Little, W. A., "The Transport of Heat Between Dissimilar Solids at Low Temperatures," *Canadian Journal of Physics*, Vol. 37, No. 3, 1959, pp. 334–349.

[11]Swartz, E. T., and Pohl, R. O., "Thermal Boundary Resistance," *Reviews of Modern Physics*, Vol. 61, No. 3, 1989, pp. 605–668.

[12]Stoner, R. J., and Maris, H. J., "Kapitza Conductance and Heat Flow Between Solids at Temperatures from 50 to 300 K," *Physical Review B: Solid State*, Vol. 48, No. 22, 1993, pp. 16,373–16,387.

[13]Morath, C. J., Maris, J. M., Cuomo, J. J., Pappas, D. L., Grill, A., Patel, V. V., Doyle, J. P., "Picosecond Optical Studies of Amorphous Diamond and Diamondlike Carbon: Thermal Conductivity and Longitudinal Sound Velocity," *Journal of Applied Physics*, Vol. 76, No. 5, 1994, pp. 2636–2640.

[14]Graebner, J. E., "Thermal Conductivity of CVD Diamond: Techniques and Results," *Diamond Films and Technology*, Vol. 3, No. 2, 1993, pp. 77–130.

[15]Stoner, B. R., Ma, G.-H. M., Wolter, S. D., and Glass, J. T., "Characterization of Bias-Enhanced Nucleation of Diamond on Silicon by in Vacuo Surface Analysis and Transmission Electron Microscopy," *Physical Review B: Solid State*, Vol. 45, No. 19, 1992, pp. 11,067–11,084.

[16]Goodson, K. E., "Thermal Conduction in Nonhomogeneous CVD Diamond Layers in Electronic Microstructures," *ASME/JSME Thermal Engineering Joint Conference*, edited by L. S. Fletcher and T. Aihara, Vol. 4, 1995, pp. 183–192.

[17]Freeman, J. J., and Anderson, A. C., "Thermal Conductivity of Amorphous Solids," *Physical Review B: Solid State*, Vol. 34, No. 8, 1986, pp. 5684–5690.

[18]Zeller, R. C., and Pohl, R. O., "Thermal Conductivity and Specific Heat of Noncrystalline Solids," *Physical Review B: Solid State*, Vol. 4, No. 6, 1971, pp. 2029–2041.

[19]Berman, R., *Thermal Conduction in Solids*, Oxford Univ. Press, Oxford, England, UK, 1976, p. 23.

[20]Heatherington, A. V., Wort, C. J. H., and Southworth, P., "Crystalline Perfection of Chemical Vapor Deposited Diamond Films," *Journal of Materials Research*, Vol. 5, No. 8, 1990, pp. 1591–1594.

[21]Goodson, K. E., Flik, M. I., Su, L. T., and Antoniadis, D. A., "Annealing-Temperature Dependence of the Thermal Conductivity of LPCVD Silicon-Dioxide Layers," *IEEE Electron Device Letters*, Vol. 14, No. 10, 1993, pp. 490–492.

[22]Goodson, K. E., "Impact of CVD Diamond Layers on the Thermal Engineering of Electronic Systems," *Annual Review of Heat Transfer*, Vol. 6, 1995, pp. 323–353.